Original Article

Institution of MECHANICAL ENGINEERS
Journal of ENGINEERING IN MEDICINE

Proc IMechE Part H:
J Engineering in Medicine
2014, Vol. 228(11) 1183–1192

DOI: 10.1177/0954411914559736
pih.sagepub.com
SAGE

Accuracy evaluation of a new stereophotogrammetry-based functional method for joint kinematic analysis in biomechanics

Maurizio Galetto[1], Laura Gastaldi[2], Giulia Lisco[2], Luca Mastrogiacomo[1] and Stefano Pastorelli[2]

Abstract

The human joint kinematics is an interesting topic in biomechanics and turns to be useful for the analysis of human movement in several fields. A crucial issue regards the assessment of joint parameters, like axes and centers of rotation, due to the direct influence on human motion patterns. A proper accuracy in the estimation of these parameters is hence required. On the whole, stereophotogrammetry-based predictive methods and, as an alternative, functional ones can be used to this end. This article presents a new functional algorithm for the assessment of knee joint parameters, based on a polycentric hinge model for the knee flexion–extension. The proposed algorithm is discussed, identifying its fields of application and its limits. The techniques for estimating the joint parameters from the metrological point of view are analyzed, so as to lay the groundwork for enhancing and eventually replacing predictive methods, currently used in the laboratories of human movement analysis. This article also presents an assessment of the accuracy associated with the whole process of measurement and joint parameters estimation. To this end, the presented functional method is tested through both computer simulations and a series of experimental laboratory tests in which swing motions were imposed to a polycentric mechanical analogue and a stereophotogrammetric system was used to record them.

Keywords

Motion analysis, biomechanics, functional methods, polycentric knee, joint parameters

Date received: 4 December 2013; accepted: 23 October 2014

Introduction

Human movement analysis is one of the main topics of biomechanics. It aims both at studying the mechanics of body motion, quantifying it and at evaluating forces acting on human joints, as well as kinematics. Thus, applied biomechanics turns to be useful in several areas like gait analysis, prosthetics and rehabilitation, ergonomics, body biodynamic and so on.

The study of human movement requires both body modeling and motion capture techniques for data acquisition. Current biomechanical models treat human body as a set of rigid bodies connected by mechanical joints. As an example, the simplest model of lower limb kinematics consists of seven motion segments: pelvis, thighs, shanks and feet, connected by six joints, like hips, knees and ankles.[1]

By means of biomechanical models, the purpose of quantitative human movement analysis is to determine and compare the position and the orientation of bone segments (i.e. motion segments of the models) involved in the motion. The relative motion can be described in terms of kinematic quantities such as joint angles, linear and angular quantities such as velocities and accelerations.

Concerning the motion capture techniques, several systems can be used for tracking human motion. Among all, optoelectronic systems are widely used for the reconstruction of human body movements. They rely on the concurrent use of a set of video-cameras

[1]Department of Management and Production Engineering (DIGEP), Politecnico di Torino, Torino, Italy
[2]Department of Mechanical and Aerospace Engineering (DIMEAS), Politecnico di Torino, Torino, Italy

Corresponding author:
Maurizio Galetto, Department of Management and Production Engineering (DIGEP), Politecnico di Torino, Corso Duca degli Abruzzi 24, 10129 Torino, Italy.
Email: maurizio.galetto@polito.it

and markers, properly attached on the body in order to be tracked. Thus, the combined use of stereophotogrammetry techniques and reflective skin markers allows to compute joint kinematics.

In detail, the video-cameras system can achieve the spatio-temporal trajectories of all the markers positioned on body segments,[2–4] so as to allow the tracking of the relative motion between different body segments. Two categories of markers can be identified: markers corresponding to specific anatomical landmarks (*anatomical markers*) and those which are instead positioned on other points (*technical markers*). To be effective, some biomechanical models require the use of anatomical markers whose positioning must respect several constraints. This may constitute a great limit especially in the case of pathological abnormalities, skin deformities, presence of prostheses or other medical devices, and so on.

Methods for joint parameters assessment

Generally, human motion patterns require the assessment of joint parameters like axes of rotation (AoRs) and centers of rotation (CoRs). This is a crucial issue due to the direct influence on the computation of both limb kinematics and dynamics. In the case of people presenting physical deformities that directly compromise motion tasks, this issue becomes even more critical. For this reason, a proper accuracy in the assessment of joint parameters is needed to guarantee reliable estimations of model parameters required for further computations, for example, clinical gait analysis.

The assessment of joint parameters can be obtained by *predictive* and *functional* methods.[5,6] Currently, laboratories for the analysis of human movement typically adopt predictive methods, which are based on regression equations experimentally obtained by investigating a certain numbers of cadavers or by means of Roentgen stereophotogrammetric analysis.[3,7,8] Using photogrammetric motion data as input, these methods define the joint parameters as functions of a proper kinematics of an anthropometric model with known number and types of degrees of freedom (DoF).

Although predictive methods are simple and immediate from an analytical point of view, they are subject to errors[9] due both to their generic approach which does not consider bony deformities or gender-based skeletal differences, and to the lack of accuracy related to the markers positioning. Protocols that employ predictive methods require the identification of specific body landmarks according to well-established models.[3,4] This is generally a difficult task, being conditioned by the amount of tissue under the skin. Also, the accuracy of the regression equations is unknown with several sets of relations available to this end.[4,9] As a consequence, predictive methods guarantee a sufficient accuracy only for few categories of people, but in most cases they are not suitable.

Functional methods are then introduced to remedy problems and limitations characterizing the predictive approaches. Relevance of these methods is mainly due to the advantages they introduce, given that they do not rely on strict protocol for markers positioning and they do not depend on the standardized anthropometric models. Differently from predictive models, they study a particular joint relying only on the information about the relative motion between those body segments connected to the joint. Several functional strategies have been proposed in the literature, allowing a classification in (1) variations of sphere fitting-based approaches[10–14] and (2) transformation techniques.[15–19] Both still require the use of at least three non-aligned markers per segment in order to define the pose of the segment itself on which they are positioned, without any constraint. The former approaches assume that each marker can rotate around the same joint axis or center with a separate arc[13,14] without any rigid body assumption. On the other hand, transformation techniques combine kinematical and geometrical constraints. They model the joint as the composition of different rigid bodies, providing joint parameters through rigid body transformations, like rotation matrices and translation vectors.[15–20] Several studies mainly based on comparative simulations using functional methods to estimate hip joint model's parameters have been proposed in the literature,[11–14,21,22] and a recent review about available algorithms[19] outlines relative pros and cons.

Generally, the validity of the assessed joint parameters is a direct consequence of the degree of congruency between the assumed mathematical model and the kinematics of the considered joint. Moreover, the best approach to precisely assess the performance of both predictive and functional method is throughout medical imaging techniques. Since, such approaches are invasive and expensive, the literature manly presents methods that have been tested using computer simulations or standard mechanical analogues.[20,23]

Purpose of a new functional method for knee joint

In human motion analysis, either using predictive or functional methods, human articulations are assumed as standard single hinge joints or monocentric spherical ones, estimating just one AoR or a CoR, respectively.[3,4,13,16,18,20] However, these assumptions represent an approximation in most cases; in particular, for the knee they lack of accuracy, due to the complex pattern of motion of this joint.

Even if physiologically the knee joint allows flexion–extension, internal–external rotation and abduction–adduction, in the literature, its kinematics is often characterized only by the flexion axis.[24–27] This is because the flexion–extension has typically the greater range of motion (RoM): during some movements, such as walking or running, the most dominant motion takes place in the sagittal plane, and hence, flexion–extension

is one of the first trends evaluated by clinicians to assess the subject motion soundness.

According to predictive methods, the flexion–extension axis is estimated as the line passing throughout the couple of anatomical markers which are fixed on the medial and lateral epicondyles,[2–4] while the knee joint center is considered as the midpoint between these markers, as shown in Figure 1. In the figure, black larger points represent anatomical markers on the knee according to predictive protocols.

On the other side, functional methods estimate the flexion–extension axis by evaluating the relative motion between shank and thigh. For this purpose, markers are freely placed on the two segments. In Figure 1, gray points are an example of a set of technical markers used for a functional protocol.

To the authors' knowledge, none of the proposed functional methods has ever assessed the effective knee joint roto-translation, due to the assumption of the joint itself as a single hinge or monocentric one. This study hence proposes a new functional algorithm specifically focusing on the knee joint kinematics: the flexion–extension axis is assumed as a mobile one, according to a polycentric kinematic model of the articulation. From a metrological point of view, this article also proposes a possible approach for the accuracy analysis of the technique used to estimate the joint parameters. This also allows to evaluate whether this functional method can be considered a viable alternative to the approaches now commonly used in the laboratories of motion analysis.

In detail, the study focuses on the algorithms implemented for data processing and analysis, with the aim of giving an estimation of the accuracy and the related uncertainty associated with the whole process of measurement.[28,29] The proposed functional method was tested using a numerical simulation and an experimental validation was also carried out by means of a phantom with a two-dimensional (2D) polycentric hinge mechanism, using its known kinematics as reference.

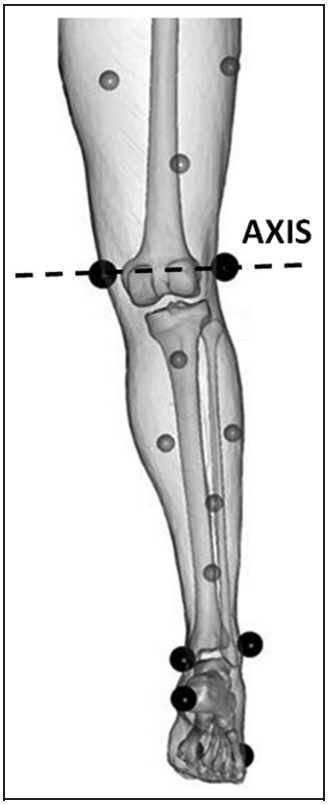

Figure 1. Example of markers positioning protocols for predictive (black points) or functional (gray points) methods and predictive flexion–extension knee axis (black dotted line).

Methodology

The most commonly used functional methods are those proposed in the literature.[13,16,18] Even if these methods present many advantages both in terms of emulation of the considered joint and of evaluation of mechanical parameters, they roughly model the kinematics of the knee joint as a simple hinge. As an alternative to these approaches, this section introduces a different model of knee joint with a movable rotation axis, in order to consider the behavior of roto-translation mainly occurring on the sagittal plane.

Polycentric knee joint model

Once established that human knee cannot be perfectly modeled as a single hinge with a fixed axis, a different functional joint model has been conceived to consider the effect of the knee roto-translation kinematics. As a first step of improvement, this section proposes a polycentric hinge model, which considers two AoR: fixed axes of rotation (fAoR) and mobile axes of rotation (mAoR), as shown in Figure 2(a).

The model is composed of three elements connected with flat hinges. Each hinge is then rigidly coupled to a cogwheel, so as to realize a gear in the center of the middle element. This allows constraining the entire movements of the three segments so that if the first element is fixed and the second one rotates of a ϑ angle with respect to its orientation, the third one rotates of the 2ϑ quantity, as shown in Figure 2(b).

A prototype realization of this functional model consists of a mechanism composed by two equal hinges rigidly fixed on three rectangular beams (see Figure 3(a) and (b)). This has also been assembled into a dummy leg model, reproducing both a thigh and a shank (see Figure 3(c)). Nominal reference features of the mechanism have been calibrated with a coordinate measuring machine (CMM—DEA Iota 0101), in order to later evaluate the trueness and the degree of precision of the proposed approach in their assessment.

New functional algorithm

Also considering the already existing methods for computing the human knee joint parameters,[10,14,15,18] a new

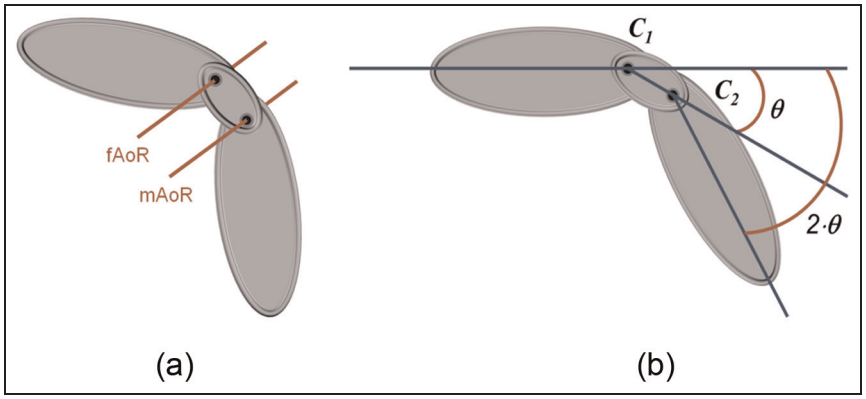

Figure 2. (a) Polycentric hinge model and (b) polycentric hinge degree of freedom.

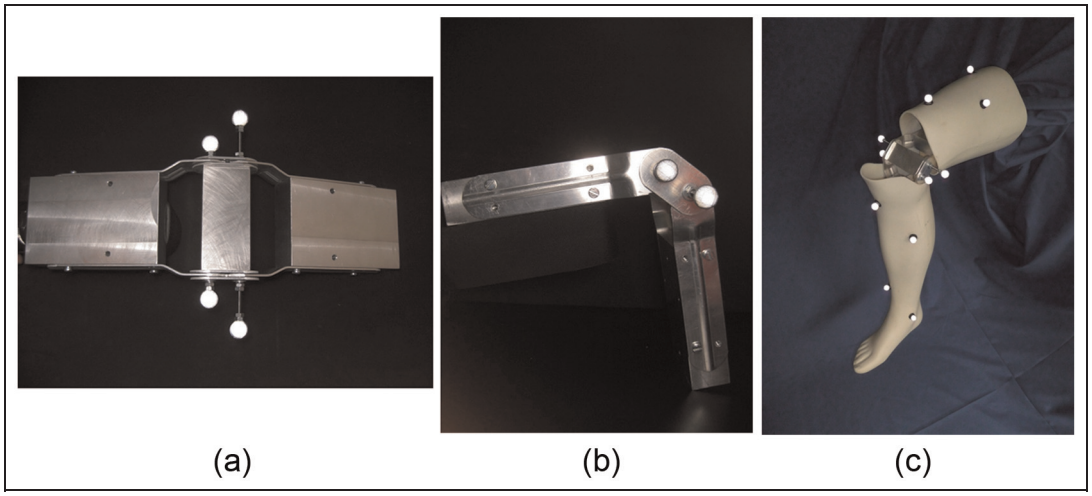

Figure 3. (a) Frontal view of the polycentric hinge, (b) side view of the polycentric hinge and (c) dummy leg model based on the mechanical polycentric hinge.

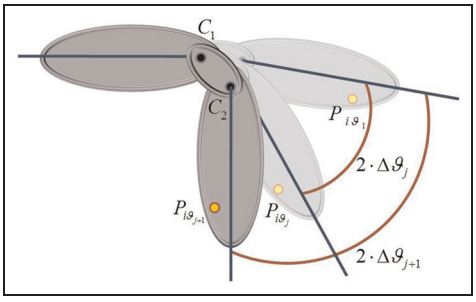

Figure 4. Scheme of joint motion in three positions and related quantities.

algorithm is here proposed, according to the polycentric hinge model.

The following approach is referred to the sagittal plane, considering the main knee motion of flexion–extension. With reference to Figure 4, for each frame (or position), the algorithm aims at assessing the two CoRs, C_1 and C_2 and their relative distance d.

The directional cosines of the two parallel AoRs can be obtained by means of the fitting approach algorithm introduced by Halvorsen et al.[13] According to this approach, the direction of the two parallel AoRs is given by the unit vector ω (see Figure 5), normal to the plane spanned by all the displacement ΔP_i of each single point (marker) P_i. This can be obtained by minimizing the following scalar product

$$s_1 = \sum_i \left(\Delta P_i^T \cdot \omega\right)^2 \tag{1}$$

This reduces to a simple quadratic optimization with the condition that the solution is a unit vector

$$\begin{aligned} s_1 &= \sum_i \left(\Delta P_i^T \cdot \omega\right)\left(\Delta P_i^T \cdot \omega\right) \\ &= \omega^T \cdot \left(\sum_i \left(\Delta P_i \cdot \Delta P_i^T\right)\right) \cdot \omega = \omega^T \cdot C \cdot \omega \end{aligned} \tag{2}$$

subject to

$$|\omega| = 1 \tag{3}$$

With reference to the notation introduced in section "Polycentric knee joint model," during each session of flexion–extension, the shank moves relative to the

Table 1. Parameters and quantities used in the algorithm.

Parameters	Description
NT	Number of markers on the thigh
NS	Number of markers on the shank
m	Number of frames for each session
$\Delta\vartheta$	Angle variation between two considered frames
C_1	Center Hinge 1 position vector
C_{20}	Center Hinge 2 position vector (initial position)
$C_{2\Delta\vartheta}$	Center Hinge 2 position vector after $\Delta\theta$ rotation
d	Vector distance between C_1 and C_2
$P_{\Delta\vartheta}$	Marker position after $\Delta\vartheta$ rotation
$R_{\Delta\vartheta}$	Roto-translation matrix for each $\Delta\vartheta$

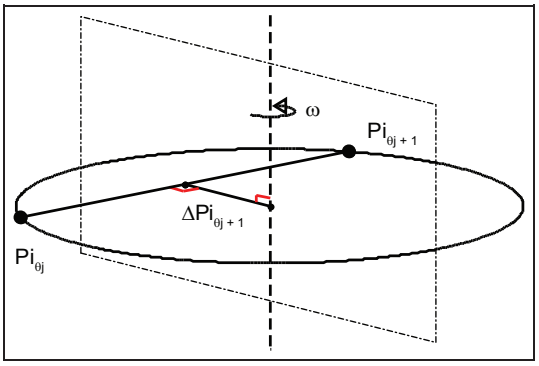

Figure 5. Scheme of the AoR. Each displacement ΔP_i of a single marker P_i is normal to the plane containing AoR.

thigh; hence, the shank rotates of $\Delta\vartheta$ respect to the intermediate element, as well of $2\cdot\Delta\vartheta$ respect to the thigh. Table 1 defines parameters and quantities used in the model.

Once spatio-temporal markers trajectories have been collected, it is possible to express the position of a marker on the shank as a roto-translation of its original position. In homogeneous coordinates, this can be formulated as follows (see Figure 4)

$$P_{i\vartheta_j} = R_{\Delta\vartheta_j}\cdot P_{i\vartheta_1} \tag{4}$$

where $i = 1,\ldots,NS$ represents the i-shank markers and $j = 1,\ldots,m$ is the j-frame of the considered motion (see Figure 5). Equation (4) can be applied for any rotation which moves a marker from its initial position to a given j position. Knowing, frame by frame, the position of each marker, the unknown parameters of matrix $R_{\Delta\vartheta}$ can be calculated. The problem can be solved by a linear least square approach, described hereafter, with the only care of avoiding matrices hill-conditioning. This can be done considering wide flexions–extensions of the leg and sufficiently large values of $\Delta\vartheta$.

In particular, the whole flexion–extension is divided into two equal parts, the first one from frame 1 to frame $m/2$, the second one from $(m/2)+1$ to m. Then two sets of $\Delta\vartheta$ values are considered, a first set is given by all the angle variations from initial position 1 to all the frames in the second part of the flexion–extension (i.e. from 1 to $(m/2)+1$, from 1 to $(m/2)+2$, until from 1 to m), the second set is given by all the angle variations from final position m to all the frames in the first part of the flexion–extension (i.e. from m to $m/2$, from m to $(m/2)-1$, until from m to 1).

Therefore, it can be demonstrated that the roto-translation matrix $R_{\Delta\vartheta_j}$ has the following structure

$$R_{\Delta\vartheta_j} = \begin{bmatrix} \cos(2\cdot\Delta\vartheta_j) & \sin(2\cdot\Delta\vartheta_j) & a_{\Delta\vartheta_j} \\ -\sin(2\cdot\Delta\vartheta_j) & \cos(2\cdot\Delta\vartheta_j) & b_{\Delta\vartheta_j} \\ 0 & 0 & 1 \end{bmatrix} \tag{5}$$

where the two translation terms include the center coordinates of C_1 (x_{C_1} and y_{C_1}) and the Euclidean components of distance d (d_x and d_y) in the initial position (1 or m respectively for the two halves of the flexion–extension)

$$\begin{aligned} a_{\Delta\vartheta_j} = & -x_{C_1}\cdot\cos(2\cdot\Delta\vartheta_j) - y_{C_1}\cdot\sin(2\cdot\Delta\vartheta_j) \\ & + d_x\cdot\left[-\cos(2\cdot\Delta\vartheta_j) + \cos(\Delta\vartheta_j)\right] \\ & + d_y\cdot\left[-\sin(2\cdot\Delta\vartheta_j) + \sin(\Delta\vartheta_j)\right] \\ b_{\Delta\vartheta_j} = & \; x_{C_1}\cdot\sin(2\cdot\Delta\vartheta_j) - y_{C_1}\cdot\cos(2\cdot\Delta\vartheta_j) \\ & + d_x\cdot\left[\sin(2\cdot\Delta\vartheta_j) + \sin(\Delta\vartheta_j)\right] \\ & + d_y\cdot\left[-\cos(2\cdot\Delta\vartheta_j) + \cos(\Delta\vartheta_j)\right] \end{aligned} \tag{6}$$

For each frame in the two halves of the flexion–extension, the corresponding roto-translation matrix $R_{\Delta\vartheta_j}$ can be evaluated using a linear least square method applied to the position values obtained for the NT markers.

This can be done by applying equation (4) to all the markers and obtaining the following expression

$$A\cdot X = l \tag{7}$$

where

$$A = \begin{bmatrix} x_{P_{1\vartheta_1}} & y_{P_{1\vartheta_1}} & 1 & 0 \\ y_{P_{1\vartheta_1}} & -x_{P_{1\vartheta_1}} & 0 & 1 \\ \vdots & \vdots & \vdots & \vdots \\ x_{P_{i\vartheta_1}} & y_{P_{i\vartheta_1}} & 1 & 0 \\ y_{P_{i\vartheta_1}} & -x_{P_{i\vartheta_1}} & 0 & 1 \\ \vdots & \vdots & \vdots & \vdots \\ x_{P_{NT\vartheta_1}} & y_{P_{NT\vartheta_1}} & 1 & 0 \\ y_{P_{NT\vartheta_1}} & -x_{P_{NT\vartheta_1}} & 0 & 1 \end{bmatrix}$$

$$X = \left(\cos(2\cdot\Delta\vartheta_j); \sin(2\cdot\Delta\vartheta_j); a_{\Delta\vartheta_j}; b_{\Delta\vartheta_j}\right)^T$$

$$l = \left(x_{P_{1\vartheta_j}}; y_{P_{1\vartheta_j}}; \ldots; x_{P_{i\vartheta_j}}; y_{P_{i\vartheta_j}}; \ldots; x_{P_{NT\vartheta_j}}; y_{P_{NT\vartheta_j}}\right)^T$$

Hence, the angle variations $\Delta\vartheta_j$ can be obtained as the following average value

$$\Delta\vartheta_j = \frac{\cos^{-1}\left(R_{\Delta\vartheta_j}(1,1)\right) + \sin^{-1}\left(R_{\Delta\vartheta_j}(1,2)\right)}{4} \tag{8}$$

Afterward, $C_1 = (\cos(2\cdot\Delta\vartheta_j); \sin(2\cdot\Delta\vartheta_j))^T$ and $d = (d_x; d_y)^T$ can be estimated by applying a linear least square method to the system of equations (6) and using

all the obtained values of $\Delta\vartheta_j$ in the first part of the flexion–extension (with $j = 1, \ldots, m/2$) and in the second part (with $j = (m/2) + 1, \ldots, m$), respectively. This particular choice of j is to ensure values of $\Delta\vartheta_j$ large enough to achieve a more robust estimate of C_1 and d.

To this aim, from equation (6), the following system can be introduced

$$\begin{cases} a_{\Delta\vartheta_j} = x_{C_1} \cdot L_{1j} + y_{C_1} \cdot L_{2j} + d_x \cdot L_{3j} + d_y \cdot L_{4j} \\ b_{\Delta\vartheta_j} = x_{C_1} \cdot L_{5j} + y_{C_1} \cdot L_{6j} + d_x \cdot L_{7j} + d_y \cdot L_{8j} \end{cases} \tag{9}$$

Also in this case, the system can be expressed in a compact form in order to have a problem like

$$A \cdot X = l \tag{10}$$

where

$$A = \begin{bmatrix} L_{11} & L_{21} & L_{31} & L_{41} \\ L_{51} & L_{61} & L_{71} & L_{81} \\ \vdots & \vdots & \vdots & \vdots \\ L_{1\frac{m}{2}} & L_{2\frac{m}{2}} & L_{3\frac{m}{2}} & L_{4\frac{m}{2}} \\ L_{5\frac{m}{2}} & L_{6\frac{m}{2}} & L_{7\frac{m}{2}} & L_{8\frac{m}{2}} \end{bmatrix}$$

$$X = \left(x_{C_1}; y_{C_1}; d_x; d_y\right)^T$$

$$l = \left(a_{\Delta\vartheta_1}; b_{\Delta\vartheta_1}; \ldots; a_{\Delta\vartheta_{\frac{m}{2}}}; b_{\Delta\vartheta_{\frac{m}{2}}}\right)^T$$

From the solution of this system obtained by the least square method, the distance between the two CoRs is obtained for the two parts of the flexion–extension

$$d = \sqrt{d_x^2 + d_y^2} \tag{11}$$

The final values of the center coordinates C_1 (x_{C_1} and y_{C_1}) and the distance d are given by the mean of the values obtained for the two parts of the flexion–extension and for the entire set of flexions–extensions acquired for the motion analysis.

Computer simulation and laboratory test

A two-step process was considered in order to test the proposed algorithm: (1) simulated analysis, to verify the algorithm behavior with inputs having different accuracies and (2) experimental analysis on empirical data recorded on the model prototype by means of a photogrammetric motion capture system designed in the Industrial Metrology and Quality Engineering Laboratories of Politecnico di Torino. Following sections will describe the details of the aforementioned phases.

Computer simulations

Preliminary computer simulations have been carried out, in order to validate the proposed algorithm. In particular, a virtual polycentric knee joint model was considered. The simulated configuration of the thigh and the shank is the one described in section "Polycentric knee joint model" and shown in Figure 2(a). According to this configuration, three markers were considered for the simulated thigh segment, while five for the simulated shank one. A reference system was fixed to the thigh segment and in particular, the x-axis was in the anterior direction, the y-axis in the lateral one and the z-axis in the superior direction. As explained before, the algorithm was conceived for a 2D analysis, on planes perpendicular to the y-axis.

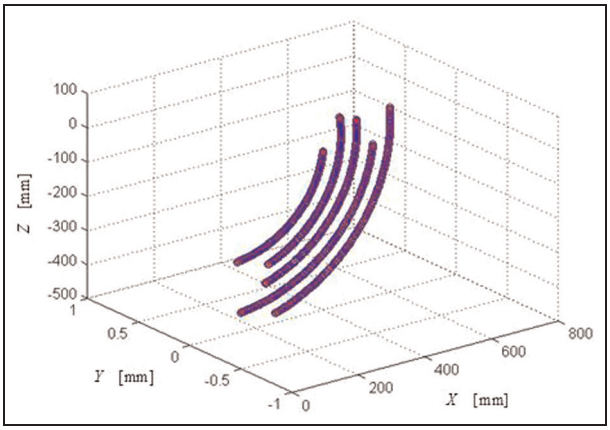

Figure 6. Example of simulated positions of the markers placed on the shank segment in swing motion.

Tests were carried out, swinging the shank respect to the fixed thigh, covering a RoM of about $\pi/2$ radians. This value was chosen lower than the full range of a physiological knee motion, since most of the human motions do not involve the full knee RoM; moreover, this value is conservative with respect to functional algorithms, since accuracy of joint parameters estimation increases with the amplitude of the motion.[18,19]

The data set shown in Figure 6 corresponds to an example of the simulated trajectories of the five markers on the shank, according to the functional marker set of Figure 1.

In order to implement and apply the algorithm, three consecutive flexions and extensions were considered for the assessment of the AoR direction, the CoRs coordinates and the distance between the two centers.

Simulations were performed in order to evaluate the influence of the uncertainty of markers positioning. To this end, a specific Gaussian noise has been applied to the generated markers data set, varying the standard deviation of the distribution itself, thus considering $\sigma = 0.1$ mm, $\sigma = 0.2$ mm, $\sigma = 0.5$ mm and $\sigma = 1$ mm. A mean squared error (MSE) has been measured to assess the accuracy of the proposed algorithm, quantifying the difference between the estimated value and the reference one. To this end, the true quantities were fixed for the coordinates of the CoR and for the distance between both centers, as $C_1 = (100; 0)$mm and $d = 24$mm, respectively. Figure 7(a)–(d) shows the histograms of the squared error E, defined as the distances

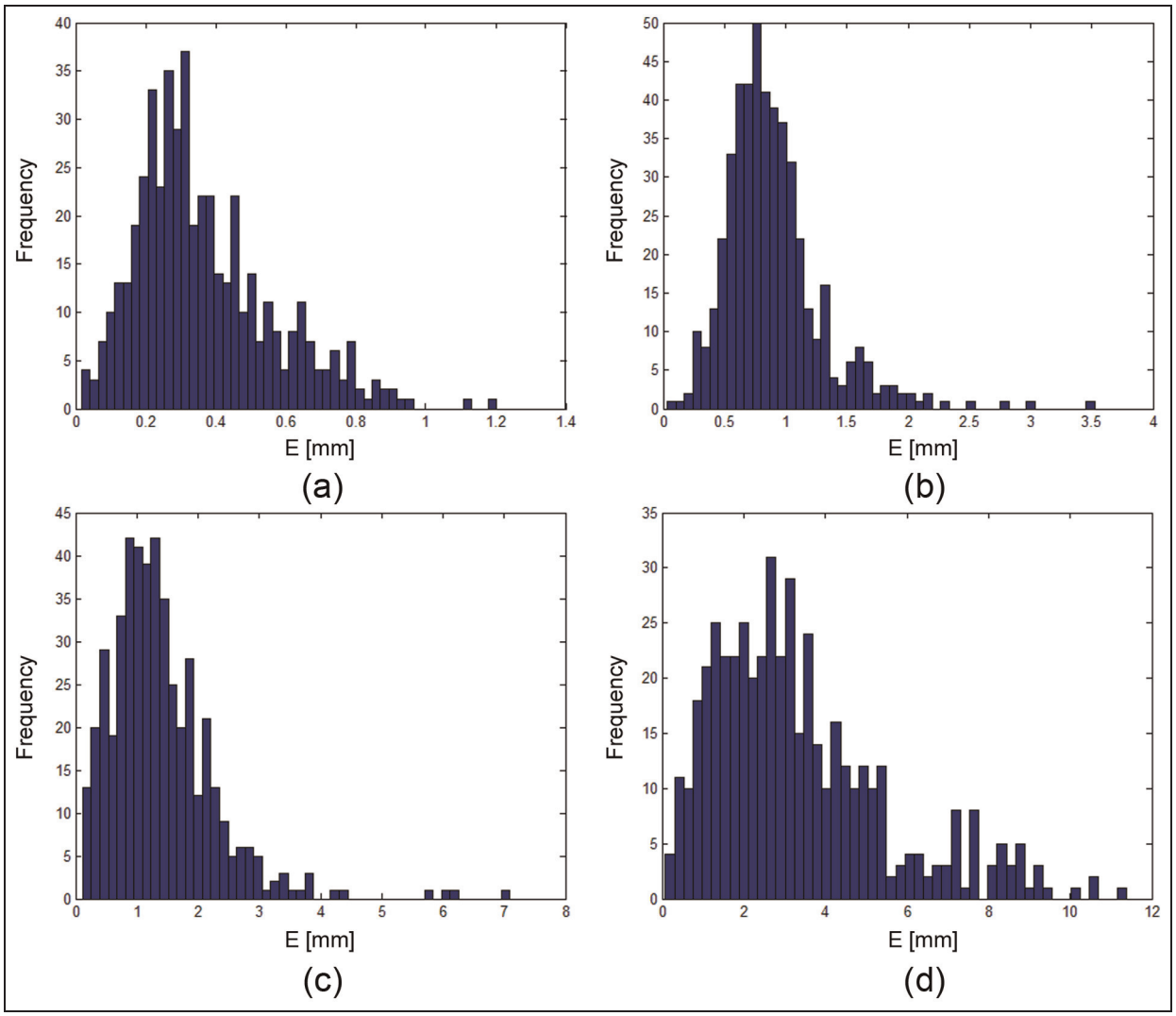

Figure 7. (a) Histogram of E values ($\sigma = 0.1$ mm), (b) histogram of E values ($\sigma = 0.2$ mm), (c) histogram of E values ($\sigma = 0.5$ mm) and (d) histogram of E values ($\sigma = 1$ mm).

between the simulated markers positions $\mathbf{x}_{s,i}$ and the respective re-calculated ones $\mathbf{x}_{c,i}$ using the estimated parameters

$$E = \sqrt{(\mathbf{x}_{s,i} - \mathbf{x}_{c,i})^2} \tag{12}$$

In detail, Figure 7(a)–(d) shows the results of E obtained with $\sigma = 0.1$ mm, $\sigma = 0.2$ mm, $\sigma = 0.5$ mm and $\sigma = 1$ mm, respectively. Results are summarized in Table 2.

Table 2. Results obtained with the simulation analysis.

Gaussian noise distribution, σ (mm)	Coordinates of CoR_1, C_1 (mm)	Distance between CoRs, d (mm)	Mean Squared Error MSE (mm)
0.1	(100.1; 0.0)	24.0	0.4
0.2	(99.6; −1.2)	24.6	1.0
0.5	(102.6; −0.2)	22.7	1.6
1	(102.9; −1.2)	30.2	4.0

Laboratory tests

To assess the performance of the proposed algorithm on a real case study, an assembled three-camera stereo-photogrammetric motion capture system was used (see Figure 8). In detail, three Hitachi KP-FD140GV cameras were used, equipped by a 1/2-in 1,450,000 pixels square lattice progressive scan charge-coupled device (CCD) and characterized by an effective resolution of 1360×1024 pixels, a maximum sample rate of 30 Hz and a shutter variable from 10 to 1/100,000 s. Each camera was also equipped with circular light-emitting diode (LED) arrays to light the measuring volume. The system was calibrated by a fully automatic single-point self-calibration technique proposed by Svoboda et al.[30] This method is able to reconstruct internal parameters besides than positions and orientations of a camera set providing an accuracy of a 10th of pixel in terms of reprojection error.

Figure 8. Layout of the photogrammetric system.

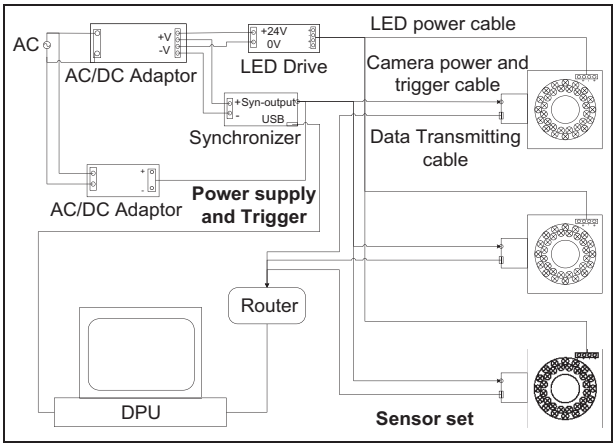

Figure 9. Connection scheme of the photogrammetric system.

A personal computer with an AMD A6-4400M CPU and 4 GB RAM was used as data processing unit (DPU). Each camera was connected to the DPU via Gigabit Ethernet cable to transmit images for data processing and real-time tracking. Furthermore, all the cameras were synchronized by a centralized trigger controlled by the same DPU. A detail of the layout of the system and the hardware connection scheme of its components is given in Figures 8 and 9, respectively.

The system—nominally able to digitize the position of a point in a space of few cubic meters with an accuracy in the order of a tenth of a millimeter—was used to replicate the simulated analysis presented in the previous section. On the dummy leg, three markers on the thigh segment and five on the shank one were freely placed, according to the functional marker set of Figure 1.

A number of three consecutive flexions and extensions sessions of the mechanism described in section "Polycentric knee joint model" were considered. In each session, a RoM of about $\pi/2$ radians was artificially produced by swinging the shank of the dummy leg respect to the thigh. For each session, the motion capture system was able to produce a scan of about 60 points for each of the five markers on the shank. At each time of the scan, a roto-translation was applied to the position of the five points on the shank so as to have a fixed reference system defined by the three points on the thigh.

Figure 10 reports the empirical distribution of the squared error $\hat{E}$, defined for each frame as the distance between the measured marker positions $\mathbf{x}_{m,i}$ and the recalculated positions using estimated parameters $\mathbf{x}_{c,i}$

$$\hat{E}_i = \sqrt{(\mathbf{x}_{m,i} - \mathbf{x}_{c,i})^2} \tag{13}$$

The average estimated parameters are $d = 26.3$ mm and $MSE = 0.7$ mm, which are compatible with the nominal distance, equal to 24.0 mm. Note that the obtained results comply with the nominal geometry of the mechanism. Also the histogram of the squared error $\hat{E}$ shows that the experimental results are consistent with the simulations (with a standard deviation of the measured points in between 0.1 and 0.2 mm).

Conclusion and future developments

In human motion analysis, the accurate assessment of joint parameters is crucially important in several fields of applications. As a consequence, the definition of the articular joint models is crucial to enhance subject-specific kinematical and dynamical analyses. Recently, several functional methods have been proposed with the aim of estimating the CoRs and the AoRs of principal human joints. While these approaches have already a clear application for the hip joint, there is a lack of application for other joints. Compared to other articulations, knee joint has indeed a complex pattern of motion which made it difficult to perfect its modeling. In this article, a first attempt to introduce a functional model that takes into account a more realistic knee joint kinematics is presented. In detail, a polycentric hinge model has been considered. This new functional algorithm gives evidence of interesting results, provided that the motion tracking system has a sufficiently high accuracy. A specific simulation proved that under a certain level of uncertainty in the measurement of markers positions (e.g. $\sigma \leqslant 0.5$mm), the proposed method produces reliable results. Such level of accuracy is normally achievable by most of the available commercial system for human motion tracking. Moreover, the simulation analysis has also demonstrated that averaging the results obtained from successive multiple flexions–extensions, the values tend to the nominal ones. That means that the larger the number of collected flexions–extensions during motion acquisition, the more reliable the parameters estimation.

Future works will further stress the analysis of the influence of the stereophotogrammetric system accuracy in order to understand the strength of the algorithm. A specific experimental plan will be designed in order to analyze the influence of a series of factors,

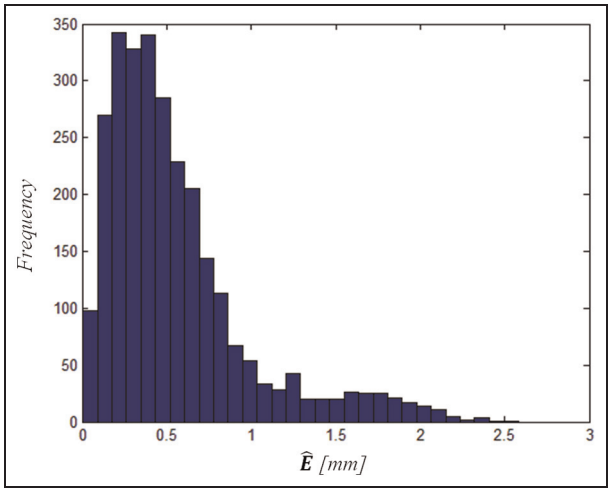

Figure 10. Histogram of *E* values for experimental analysis.

which may affect the correct behavior of the algorithm, such as the number of markers, the extent of flexion–extension, the number of consecutive flexions and extensions, the number of frames in each session and so on.

Moreover, current model enhancement will be necessary to allow its use in a wider context of applications, for example, directly during walking. Further studies will address the design of a three-dimensional (3D) knee joint functional model, also considering abduction–adduction and internal–external rotations.[31]

Declaration of conflicting interests

The authors declare that there is no conflict of interest.

Funding

This research received no specific grant from any funding agency in the public, commercial or not-for-profit sectors.

References

1. Hatze H. A mathematical model for the computational determination of parameter values of anthropomorphic segments. *J Biomech* 1980; 13(10): 833–843.
2. Cappozzo A, Della Croce U, Leardini A, et al. Human movement analysis using stereophotogrammetry. Part 1: theoretical background. *Gait Posture* 2005; 21: 186–196.
3. Davis RB, Ounpuu S, Tyburski D, et al. A gait analysis data collection and reduction technique. *Hum Mov Sci* 1991; 10(5): 575–587.
4. Kadaba MP, Ramakrishnan HK and Wootten ME. Measurement of lower extremity kinematics during level walking. *J Orthop Res* 1990; 8: 383–392.
5. Cappozzo A, Catani F, Leardini A, et al. Position and orientation in space of bones during movement: experimental artefacts. *Clin Biomech* 1996; 11(2): 90–100.
6. Leardini A, Chiari L, Della Croce U, et al. Human movement analysis using stereophotogrammetry. Part 3. Soft tissue artifact assessment and compensation. *Gait Posture* 2005; 21(2): 212–225.
7. Seidel GK, Marchinda DM, Dijkers M, et al. Hip joint center location from palpable bony landmarks—a cadaver study. *J Biomech* 1995; 28(8): 995–998.
8. Kirkwood RN, Culham EG and Costigan P. Radiographic and non-invasive determination of the hip joint center location: effect on hip joint moments. *Clin Biomech* 1999; 14: 227–235.
9. Bell AL, Petersen DR and Brand RA. A comparison of the accuracy of several hip centre location prediction methods. *J Biomech* 1990; 23: 617–621.
10. Cappozzo A. Gait analysis methodology. *Hum Mov Sci* 1984; 3: 27–50.
11. Leardini A, Cappozzo A, Catani F, et al. Validation of a functional method for the estimation of hip joint centre location. *J Biomech* 1999; 32: 99–103.
12. Piazza SJ, Okita N and Cavanagh PR. Accuracy of the functional method of hip joint center location: effects of limited motion and varied implementation. *J Biomech* 2001; 34(7): 967–973.
13. Halvorsen K, Lesser M and Lundberg A. A new method for estimating the axis of rotation and the center of rotation. *J Biomech* 1999; 32: 1221–1227.
14. Gamage SSHU and Lasenby J. New least squares solutions for estimating the average centre of rotation and the axis of rotation. *J Biomech* 2002; 35: 87–93.
15. Woltring HJ, Huiskes R, De Lange A, et al. Finite centroid and helical axis estimation from noisy landmark measurements in the study of human joint kinematics. *J Biomech* 1985; 18(5): 379–389.
16. Spoor CW and Veldpaus FE. Rigid body motion calculated from spatial coordinates of markers. *J Biomech* 1980; 13: 391–393.
17. Soderkvist I and Wedin PA. Determining the movements of the skeleton using well-configured markers. *J Biomech* 1993; 26: 1473–1477.
18. Ehrig RM, Taylor WR, Duda GN, et al. A survey of formal methods for determining the centre of rotation of ball joints. *J Biomech* 2006; 39: 2798–2809.
19. Ehrig RM, Taylor WR, Duda GN, et al. A survey of formal methods for determining functional joint axes. *J Biomech* 2007; 40: 2150–2157.
20. Schwartz MH and Rozumalski A. A new method for estimating joint parameters from motion data. *J Biomech* 2005; 38: 107–116.
21. Sangeux M, Peters A and Baker R. Hip joint centre localization: evaluation on normal subjects in the context of gait analysis. *Gait Posture* 2011; 34: 324–328.
22. Camomilla V, Cereatti A, Vannozzi G, et al. An optimized protocol for hip joint centre determination using the functional method. *J Biomech* 2006; 39(6): 1096–1106.
23. MacWilliams BA. A comparison of four functional methods to determine centers and axes of rotations. *Gait Posture* 2008; 28: 673–679.
24. Churchill DL, Incavo SJ, Johnson CC, et al. The transepicondylar axis approximates the optimal flexion axis of the knee. *Clin Orthop Relat Res* 1998; 356: 111–118.
25. Li G, Most E, Otterberg E, et al. Biomechanics of posterior-substituting total knee arthroplasty: an in vitro study. *Clin Orthop Relat Res* 2002; 404: 214–225.
26. Most E, Axe J, Rubash H, et al. Sensitivity of the knee joint kinematics calculation to selection of flexion axes. *J Biomech* 2004; 37: 1743–1748.
27. Asano T, Akagi M and Nakamura T. The functional flexion-extension axis of the knee corresponds to the

surgical epicondylar axis: in vivo analysis using a biplanar image-matching technique. *J Arthroplasty* 2005; 20: 1060–1067.
28. Luhmann T, Robson S, Kyle S, et al. *Close range photogrammetry*. New York: John Wiley & Sons, 2006.
29. JCGM 100:2008. *Evaluation of measurement data—guide to the expression of uncertainty in measurement*. Geneva: International Organization for Standardization.
30. Svoboda T, Martinec D and Pajdla T. A convenient multi-camera self-calibration for virtual environments. *Presence* 2005; 14(4): 407–422.
31. Nording M and Frankel VH. *Basic biomechanics of the musculoskeletal system*. 3rd ed.Mexico Federal District, Mexico: McGraw-Hill Interamericana, 2005.